Resonantly enhanced spin-lattice relaxation of Mn^{2+} ions in diluted magnetic (Zn,Mn)Se/(Zn,Be)Se quantum wells

J. Debus,[1,*] V. Yu. Ivanov,[2] S. M. Ryabchenko,[3] D. R. Yakovlev,[1,4] A. A. Maksimov,[5] Yu. G. Semenov,[6] D. Braukmann,[1] J. Rautert,[1] U. Löw,[7] M. Godlewski,[2] A. Waag,[8] and M. Bayer[1,4]

[1]*Experimentelle Physik 2, Technische Universität Dortmund, 44227 Dortmund, Germany*

[2]*Institute of Physics, Polish Academy of Sciences, 02668 Warsaw, Poland*

[3]*Institute of Physics, NAS of Ukraine, 03028 Kiev, Ukraine*

[4]*Ioffe Institute, Russian Academy of Sciences, 194021 St. Petersburg, Russia*

[5]*Institute of Solid State Physics, Russian Academy of Sciences, 142432 Chernogolovka, Russia*

[6]*Department of Electrical and Computer Engineering, North Carolina State University, Raleigh, North Carolina 27695, USA*

[7]*Theoretische Physik 1, Technische Universität Dortmund, 44227 Dortmund, Germany*

[8]*Institute of Semiconductor Technology, University of Braunschweig, 38106 Braunschweig, Germany*

(Received 9 December 2015; revised manuscript received 29 March 2016; published 10 May 2016)

The dynamics of spin-lattice relaxation in the magnetic Mn^{2+} ion system of (Zn,Mn)Se/(Zn,Be)Se quantum-well structures are studied using optical methods. Pronounced cusps are found in the giant Zeeman shift of the quantum-well exciton photoluminescence at specific magnetic fields below 10 T, when the Mn spin system is heated by photogenerated carriers. The spin-lattice relaxation time of the Mn ions is resonantly accelerated at the cusp magnetic fields. Our theoretical analysis demonstrates that a cusp occurs at a spin-level mixing of single Mn^{2+} ions and a quick-relaxing cluster of nearest-neighbor Mn ions, which can be described as intrinsic cross-relaxation resonance within the Mn spin system.

DOI: 10.1103/PhysRevB.93.195307

I. INTRODUCTION

Semiconductor nanostructures with randomly distributed magnetic ions show highly promising spin-electronic functionalities with regard to collective spin ordering [1–4]. In that context, diluted magnetic semiconductors (DMSs) with their great potential of efficient spin injection and magnetization manipulation by optical methods are treated nowadays as model materials for spin-electronics [5–11]. The optical, electronic, and magnetic properties of DMSs and their heterostructures are determined by three coupled systems: magnetic ions, carriers (electrons and holes), and phonons. The spin and energy transfer between them leads to a great variety in the spin dynamics of carriers and magnetic ions, whose concentrations mainly modify the dynamics [12]. In, for instance, II-VI structures doped with Mn^{2+} ions, the carrier spin relaxation falls in the subpicosecond range, the formation of magnetic polarons occurs during 50–200 ps, and the spin-lattice relaxation of the Mn ions covers the temporal range from nano- to milliseconds [13–16]. However, the picture of the involved mechanisms is far from complete.

The spin-lattice relaxation (SLR) of single Mn^{2+} ions is limited, as they only weakly interact with the lattice [17,18], while in Mn spin clusters the SLR is very efficient [19]. The ensemble of Mn ions in a nonequilibrium magnetic state can relax to their equilibrium state via the clusters by transferring spin and energy to them. In II-VI DMSs, the Mn spins in clusters are coupled antiferromagnetically, and Mn ion pairs, in particular, have zero magnetic moment in the singlet ground state [20]. Therefore, the paramagnetic single Mn ions mainly contribute to the magneto-optical effects in DMSs, while the Mn clusters control the spin dynamics. Phenomenologically, these aspects explain the strong dependence of the SLR time on the concentration of the Mn ions. But, the underlying mechanisms need to be clarified to extend the general theory of magnetization relaxation as well as to enhance the practical usage of DMSs. Besides perspectives for DMS materials, details on the magnetization transfer from paramagnetic centers to quick-relaxing centers concerning the spin-diffusion mechanism of the SLR are also relevant for the paramagnetic relaxation theory.

In this article, we demonstrate the resonantly enhanced spin transfer between single Mn ions and Mn clusters in (Zn,Mn)Se/(Zn,Be)Se quantum wells (QWs) by optically controlling the Mn spin temperature. The giant Zeeman shift of the exciton photoluminescence energy significantly deviates from the modified Brillouin function at specific magnetic fields below 10 T. The differences correspond to reductions in the spin temperature of the Mn spin system that needs to be heated by, e.g., photocarriers and originate from the fastening of the magnetization relaxation, which is evidenced by pump-probe measurements of the spin-lattice relaxation time. In our theoretical model, the spin-lattice relaxation is accelerated at certain magnetic fields due to the mixing between spin levels of single Mn^{2+} ions and quick-relaxing pairs of primarily nearest-neighbor Mn^{2+} ions. At these intrinsic cross-relaxation resonances, spin is transferred highly efficiently from the ensemble of single Mn ions to Mn clusters without any energy exchange with the phonon bath.

II. EXPERIMENTAL DETAILS

We have studied four $Zn_{1-x}Mn_xSe/Zn_{0.94}Be_{0.06}Se$ QW structures with $x = 0.004$ (no. 1), 0.012 (no. 2), 0.020 (no. 3), and 0.035 (no. 4) and type-I band alignment. The samples were

*Author to whom all correspondence should be addressed: joerg.debus@tu-dortmund.de

grown by molecular-beam epitaxy on (100)-oriented GaAs substrates. Samples no. 1 and no. 2 contain five 10-nm-thick (Zn,Mn)Se QWs separated by 20-nm-thick (Zn,Be)Se barriers, while the two other samples have a single QW. All samples are nominally undoped; hence, the background carrier densities in the QWs are considerably less than 10^{10} cm^{-2}. The conclusions on the Mn spin properties studied for the QW structures can also be drawn for bulk samples and quantum dots, while in QW structures higher carrier densities as well as spatially more homogeneous carrier distributions can be achieved by optical excitation.

The samples were studied by stationary and time-resolved photoluminescence (PL). They were immersed in pumped liquid helium at a temperature of $T = 1.8$ K and exposed to magnetic fields B up to 10 T that were applied in Faraday geometry parallel to the structure growth z axis. For the excitation of the stationary PL, a semiconductor laser with 3.06 eV photon energy in continuous-wave (CW) mode was used. The time-integrated PL with high spectral resolution was measured with a liquid-nitrogen-cooled charge-coupled-device (CCD) camera combined with a triple-monochromator [21]. The dynamics of the Mn spin system were measured using a pump-probe technique [22]. The sample was excited by 5 ns pump pulses (3.49 eV), while changes in the Mn spin temperature were measured by the energy shift of the exciton PL line probed by weak laser pulses of the semiconductor laser whose durations were adjusted to a few tens of microseconds [23]. A gated CCD camera with a time resolution of 2 ns, connected to a 0.5 m monochromator, was used for time-resolved PL detection.

III. CUSP DETECTION VIA STATIONARY AND TIME-RESOLVED PHOTOLUMINESCENCE

The QW PL of sample no. 2 is shown in the inset of Fig. 1(a). The exciton (X) PL measured at $B = 0$ and 4 T differs strongly in energy due to the giant Zeeman splitting. The main panel shows the magnetic-field dependence of the exciton PL peak energy, $E_X(B)$, for three excitation densities. The overall trend of the decreasing E_X with increasing field can be described by the well-known modified Brillouin function: $E_X \propto x S_{eff}(x)\, B_{5/2}\{\frac{5 g_{Mn}\mu_B B}{2k_B[T_0(x)+T_{Mn}]}\}$. The g factor of the Mn^{2+} ion with spin 5/2 is given by $g_{Mn} = 2.0$, μ_B is the Bohr magneton, and k_B is the Boltzmann constant [24]. $T_0(x) > 0$ is the effective paramagnetic Curie temperature, and $S_{eff}(x)$ is the effective Mn spin; both are used for a phenomenological description of the antiferromagnetic exchange interaction between neighboring Mn ions. From the fit of the data points (black circles) measured at a low laser density of 6 mW/cm^2, where the Mn spin temperature T_{Mn} can be set equal to the helium bath temperature, $T_0 = 0.92$ K and $S_{eff} = 2.14$ are assessed for sample no. 2 with $x = 0.012$. By fixing these parameters, the Mn spin temperature at a high pump power is evaluated from the fitting of the $E_X(B)$ dependence.

As one can see in Fig. 1(a), $E_X(B)$ increases for high excitation power densities; T_{Mn} rises to 2.8 K for $P = 0.7$ W/cm^2, and to 7.9 K for 8.8 W/cm^2. Here, the Mn spin temperature is controlled by the balance between the heating of the Mn spin system via hot photocarriers and its cooling through the SLR. A surprising and remarkable observation is

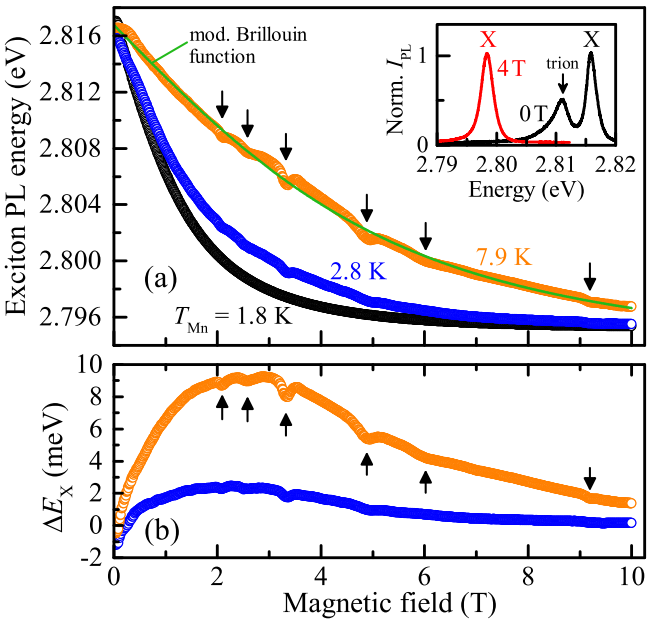

FIG. 1. (a) Giant Zeeman shift of the exciton PL energy for sample no. 2 measured at different CW excitation powers 6 mW/cm^2 ($T_{Mn} = 1.8$ K), 0.7 W/cm^2 (2.8 K), and 8.8 W/cm^2 (7.9 K); $T = 1.8$ K. The cusp positions are marked by arrows. Inset: normalized PL spectra for $B = 0$ and 4 T; $P = 0.7$ W/cm^2. (b) Difference of the exciton energies, $E_X(T_{Mn}) - E_X(1.8\text{ K})$, for $P = 0.7$ and 8.8 W/cm^2 shown by blue and orange, respectively.

that, for the heated Mn spin system, the exciton PL energy is significantly reduced at specific magnetic fields: 2.09, 2.58, 3.32, 4.88, 6.02, and 9.19 T. These cusps, which highlight strong deviations from the modified Brillouin function behavior [see the green solid curve in Fig. 1(a)], are more pronounced in Fig. 1(b), where the field dependences of the energy differences $\Delta E_X = E_X(T_{Mn}) - E_X(1.8\text{ K})$ are shown. The strongest change in ΔE_X is observed at 3.32 T, where the cusp amplitude $A_{cusp} = |\delta E(3.32\text{ T})| = |\Delta E_X(3.32\text{ T}) - \Delta E_X(3.0\text{ T})|$ reaches 0.8 meV at 8.8 W/cm^2. The giant redshift of the exciton PL line at this magnetic field is reduced due to the heating of the Mn spin temperature to 7.9 K under the 8.8 W/cm^2 excitation. Accordingly, the value of 0.8 meV corresponds to a restoration of the Mn spin temperature by about 0.8 K.

The excitation density dependence of A_{cusp} is shown by the black circles in Fig. 2(a). For weak CW laser power densities below 0.2 W/cm^2, the amplitude is considerably small (<0.1 meV). It reaches a maximum value of 0.8 meV at 8.8 W/cm^2, and for higher excitation densities the cusp becomes more shallow. The cusp is only observed when the Mn spin temperature T_{Mn} is larger than the lattice temperature T, i.e., when through the optically excited carriers the Mn spin system is heated above the phonon bath temperature; see the triangles in Fig. 2(a). It decreases the giant Zeeman shift of the exciton PL line that correspondingly shifts to higher energies. Here, T_{Mn} has been estimated from fitting the modified Brillouin function to the exciton energy measured from 3 to 4 T. At high optical excitation power density ($P > 15$ W/cm^2), the cusp amplitude decreases remarkably. Since the cusp

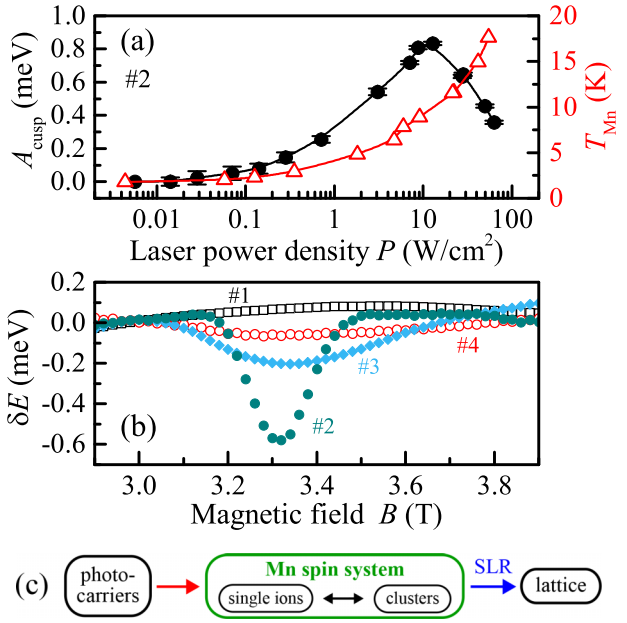

FIG. 2. (a) CW laser-power density dependence of the 3.32-T-cusp amplitude (closed circles) and Mn spin temperature (open triangles, right scale); sample no. 2, $T = 1.8$ K. Lines are guides for the eye. (b) Energy difference $\delta E(B)$ for the 3.32-T cusp for the four samples studied; $P = 3$ W/cm^2. (c) Scheme of interactions: the Mn spin system is heated by photocarriers and mainly cooled via Mn clusters to the lattice temperature.

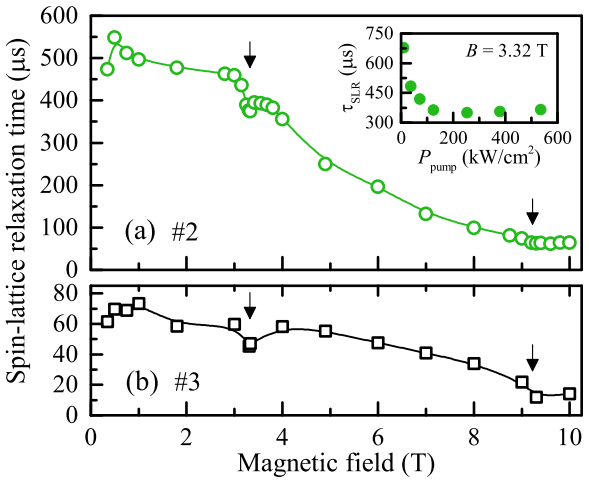

FIG. 3. SLR time as a function of the magnetic field for sample no. 2, $x = 0.012$ (a), and no. 3, $x = 0.020$ (b); $T = 1.8$ K. The error of τ_{SLR} does not exceed the symbol size. Inset: pump power dependence of τ_{SLR}.

amplitude at a fixed magnetic field depends on the difference $T_{Mn} - T$, the decrease may be caused by a local heating of the phonon system above the helium temperature of 1.8 K. Note that the width of the cusp resonance is not changed significantly over the whole range of power densities applied.

The cusp fields do not depend on the Mn concentration, as is shown, exemplarily for the 3.32-T cusp, in Fig. 2(b), although sample no. 1 with lowest x does not show a minimum in $E_X(B)$ at the chosen experimental conditions. For increasing x, the cusps broaden with shallow flanks at high fields, and the cusp amplitude changes nonmonotonically, having a maximum for $x = 0.012$. It is worthwhile mentioning that the cusps are observed in both multiple- and single-QW structures, thus allowing us to exclude a possible participation of folded acoustic phonons in the cusp appearance, which might be present in multiple QWs. A cusp at 3.32 T has also been observed in an n-doped $Zn_{0.988}Mn_{0.012}Se$/(Zn,Be)Se QW.

According to the scheme of Fig. 2(c), it is consequential to suggest that the cusps are attributed to a cooling of the heated Mn spin system that is provided at specific magnetic fields by a resonant spin transfer from single Mn^{2+} ions to Mn clusters, resulting in accelerated spin-lattice dynamics. This is confirmed by direct measurements of the SLR time τ_{SLR}, shown in Fig. 3 for samples no. 2 and no. 3. τ_{SLR} was evaluated by probing the temporal decay of the exciton PL after an intense pump pulse with 105 kW/cm^2 [22]. At 3.3 and 9.2 T, the SLR time is reduced by about 20%, reflecting the cusp profile measured in the time-integrated giant Zeeman shift. The dependence of the SLR time on the pump density is depicted in the inset of Fig. 3(a) for $B = 3.32$ T. With increasing P_{pump}, τ_{SLR} speeds up from 700 to 350 μs and saturates at this level for $P_{pump} > 100$ kW/cm^2.

IV. THEORETICAL MODELING OF CUSP RESONANCES

The SLR of paramagnetic centers in crystals through quick-relaxing clusters is well known: energy is carried from a heated paramagnetic ion to the vicinity of a quick-relaxing center via the spin-diffusion mechanism, and after that it is transferred to the center. When the mechanism of this transfer includes cross-resonances between spin levels, it can be a resonant process. The resonant character of the SLR acceleration shall be explained by the mixing of spin levels in a complex of magnetic ions leading to anticrossings, and thus the spin and energy transfer from the paramagnetic single ions to the quick-relaxing clusters does not require the energy exchange (absorption or emission) with the phonon system, which would otherwise slow down the relaxation process. The simplest complex consists of a single Mn spin and a pair of nearest-neighbor (NN) Mn spins, which are coupled antiferromagnetically and form six multiplets with total spins $S_{pair} = 0,1,2,\ldots,5$ [20]. In the presence of state mixing at a crossing point, resonant spin transfer takes place when the splitting of the single-ion spin states with different S_z corresponds to the splitting between the pair state with $S_{pair} = 0$ and the component with lowest $S_{pair,z}$ of the pair state with $S_{pair} = 1$. By neglecting interactions between the single ion and the pair cluster, the respective resonance fields are $B_n = \frac{2J_{NN}}{n\, g_{Mn}\mu_B}$, $n = 1,2,\ldots,6$, where $2J_{NN}$ denotes the zero-field energy splitting between the above-mentioned pair states with the constant $J_{NN} \equiv J_{12} = -(1.05\text{–}1.12)$ meV of the isotropic exchange interaction between the paired ions [25]. This equation qualitatively describes the cusp fields. For additional analysis, we consider magnetic dipole-dipole coupling, crystal fields of cubic and axial symmetry, anisotropic exchange, and Dzyaloshinsky-Moriya interaction inside the pair and between the single spin and paired ions. The latter two interactions provide a fast relaxation of magnetic moments [26,27].

The total Hamiltonian, which is used for the calculations of the spin-level structures for a Mn complex, reads

$$\hat{H} = \hat{H}_{\mathrm{Z}} + \hat{H}_{\mathrm{iso}} + \hat{H}_{\mathrm{dip}} + \hat{H}_{\mathrm{ani}} + \hat{H}_{\mathrm{DM}} + \hat{H}_{\mathrm{cub}} + \hat{H}_{\mathrm{ax}}. \quad (1)$$

The analysis of the spin-level structure is conceptually based on two points: (i) Calculation of the magnetic fields, where spin levels with different $S_{\mathrm{total},z}$ cross each other. This is essential, but not a sufficient condition for the modeling of the cusp resonance fields. At these fields, cross-relaxation may take place without energy dissipation to the phonon system. (ii) Determination of the spin-level mixing at the corresponding magnetic fields; the mixing results in level anticrossing.

The Zeeman interaction of the Mn spins

$$\hat{H}_{\mathrm{Z}} = g_{\mathrm{Mn}}\mu_{\mathrm{B}} B_z \sum_i S_{z,i} \quad (2)$$

for a magnetic field **B** applied along the QW growth axis **z**, and the isotropic exchange

$$\hat{H}_{\mathrm{iso}} = -2\sum_{i>j} J_{ij}(\mathbf{S}_i\mathbf{S}_j), \quad (3)$$

which couples the NN ions of a pair cluster antiferromagnetically (negative exchange constant), form the energies of the levels and are mainly responsible for the unperturbed level crossings. The isotropic exchange interaction does not contribute to SLR due to the commutation of its Hamiltonian with $\hat{H}_{\mathrm{Z}}$. The indices i and j denote a Mn ion of the complex considered. The three-dimensional Mn-ion spin vector **S** contains the components $S_{x'}$, S_y, and S_z, where x', y, and z describe the local cubic axes of the nearest tetrahedron of each magnetic ion.

The dipole-dipole interaction between the Mn ions with distance vector **R**,

$$\hat{H}_{\mathrm{dip}} = \frac{g_{\mathrm{Mn}}^2\mu_{\mathrm{B}}^2}{R^3}\sum_{i>j}\left[\mathbf{S}_i\mathbf{S}_j - 3\frac{(\mathbf{RS}_i)(\mathbf{RS}_j)}{R^2}\right], \quad (4)$$

and the anisotropic exchange with the constants $\alpha_{ij} + \beta_{ij} + \gamma_{ij} = 0$ as well as the Dzyaloshinsky-Moriya interaction,

$$\hat{H}_{\mathrm{ani}} = \sum_{i>j}(\alpha_{ij}S_{x',i}S_{x',j} + \beta_{ij}S_{y,i}S_{y,j} + \gamma_{ij}S_{z,i}S_{z,j}), \quad (5)$$

$$\hat{H}_{\mathrm{DM}} = \sum_{i>j}\mathbf{D}_{ij}(\mathbf{S}_i \times \mathbf{S}_j), \quad (6)$$

are of key importance for the spin-level mixing, while they also lead to small corrections in the level energies. The dipolar interaction is weak in comparison to $\hat{H}_{\mathrm{ani}}$ and $\hat{H}_{\mathrm{DM}}$, which are present inside a NN pair as well as between the paired and single ions. $\hat{H}_{\mathrm{ani}}$ ($\hat{H}_{\mathrm{DM}}$) yields nondiagonal matrix elements between the states with even (odd and even) $\Delta S_{\mathrm{total},z}$. The direction of the vectorial constant $\mathbf{D}_{ij}$ is determined by the properties of the electron-shell orbitals of the Mn ions i and j participating in the interaction; it is perpendicular to the plane that includes the ions i and j as well as the adjacent anion. For the calculations, $D = 15$ μeV is used [26]. Each cation in the sphalerite structure of ZnSe has 12 nearest-neighboring cation positions. The radius vectors connecting the NN cation positions can enclose three different angles with the z axis given by $\pi/4$, $\pi/2$, and $3\pi/4$. The main axes of the $\hat{H}_{\mathrm{ani}}$ and $\hat{H}_{\mathrm{DM}}$ interactions are connected to the pair radius-vector direction. The pairs with $\pi/4$ and $3\pi/4$ orientations of the radius vector are equivalent to each other with respect to the magnetic-field direction, while they differ from the pairs with $\pi/2$. This leads to level splittings of two different types of NN pairs in a magnetic field.

Moreover, we consider the cubic and axial crystal fields through the Hamiltonians

$$\hat{H}_{\mathrm{cub}} = a\sum_i\left(S_{x',i}^4 + S_{y,i}^4 + S_{z,i}^4\right), \quad (7)$$

$$\hat{H}_{\mathrm{ax}} = \Lambda_{\mathrm{ax}}\sum_i S_{z,i}^2. \quad (8)$$

The value $a = 0.23$ μeV that corresponds to 0.002 T for the cubic crystal field is taken from Ref. [28]. The axial crystal-field term of $\Lambda_{\mathrm{ax}}S_z^2$-type arises in the spin Hamiltonian, since stress is directed along the QW growth direction, although ZnSe has a cubic (sphalerite) crystal structure. This term results in a small splitting of the zero-field spin states with different $|S_z|$ and in a nonequidistant Zeeman splitting of spin states with different S_z. The Λ_{ax} value is -5.7 μeV ($\widehat{=} -0.05$ T) [29].

The calculated spin levels for the complex of a NN pair weakly coupled to a single Mn ion are shown in Fig. 4(a); the exchange constants J_{13} and J_{23} are set to -8.5 μeV [30]. One clearly sees the spin levels of the multiplet, whose total spin $S_{\mathrm{total},z}$ is governed by $S_{\mathrm{pair}} = 0$ and $S_z = 5/2, \ldots, -5/2$, and at high energies that of the multiplets, whose $S_{\mathrm{total},z}$ values

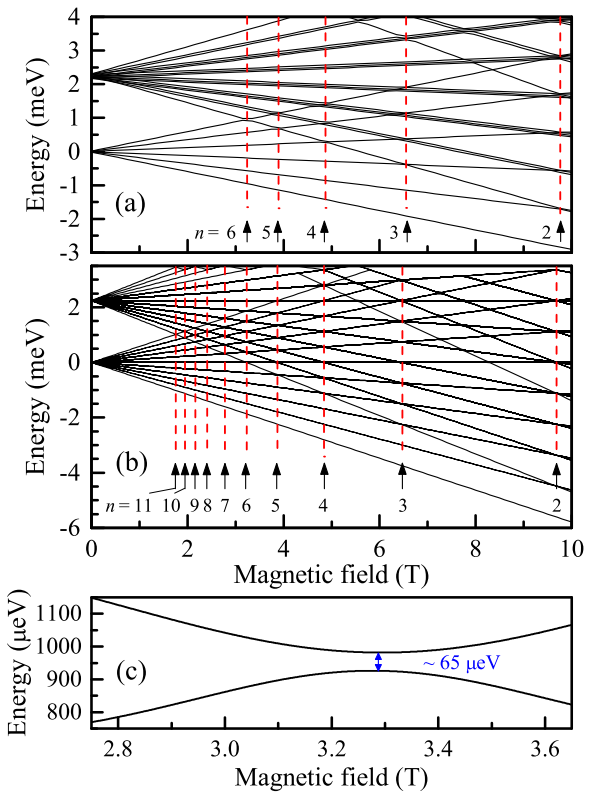

FIG. 4. Calculated energies of spin levels as a function of the magnetic field for two complexes of Mn^{2+} ions: one (a) and two (b) single Mn ions interacting with a NN pair; $J_{\mathrm{NN}} = -1.10$ meV. (c) Enlarged view of the level anticrossing, $n = 6$, for a complex of four Mn spins.

result from combining the states with $S_{\text{pair}} = 1$ and different S_z. The magnetic fields, at which cusps are expected due to mixed states that are accompanied by level anticrossings, are marked by red dashed lines and arrows. The selection rules of the state mixing are given by $\Delta S_{\text{pair}} = 1$ and $\Delta S_{\text{total},z} > 0$, where $\Delta S_{\text{total},z} \equiv n$ is the difference in the total spin projection values of the whole complex [31]. Level anticrossings for $\Delta S_{\text{total},z}$ from 6 down to 2 occur at 3.29, 3.74, 4.71, 6.39, and 9.60 T. They are in good agreement with the experiment; see Fig. 1(b). However, the cusps at lower magnetic fields ($B < 3$ T) cannot be explained within the frame of the three Mn-spin complex.

The experimentally observed low-field cusps can be described by a complex containing a NN pair that is weakly coupled to two single weakly interacting Mn ions, where the exchange strengths are estimated at -8.5 μeV. The respective results, shown in Fig. 4(b), demonstrate resonance fields at 1.76, 1.94, 2.15, 2.41, and 2.79 T for $11 \geqslant \Delta S_{\text{total},z} \geqslant 7$. The level repulsion of the anticrossings, which reflects the interaction strength between the spin levels as well as the spin-transfer efficiency, amounts to a few tens of μeV; the level anticrossing at 3.29 T is shown in Fig. 4(c). The good agreement between experiment and theory allows us to conjecture that such complexes of two single Mn ions and a NN pair are sufficient to simulate, for small x, the ensemble of mutually interacting Mn spins.

The NN pairs have the highest cluster formation probability for small x; nevertheless, next-nearest-neighbor (NNN) pairs are also present [32]. Level anticrossings related to NNN pairs, whose exchange constant was approximated to $J_{\text{NNN}} = (-0.26 \pm 0.21)$ meV [33], fall close to the 3.32-T cusp. One may suppose that this cusp is also contributed by the interaction of single ions with a NNN pair for $\Delta S_{\text{total},z} = 1$ or 2 in consideration of fluctuating rhombic crystal fields in addition to the dipolar and exchange interactions. However, complexes including triplet clusters of NN Mn^{2+} have anticrossings with weak level repulsion for $\Delta S_{\text{pair}} = 1$ and $\Delta S_{\text{total},z} > 0$ at distinctly different magnetic fields. Moreover, the different triplet-cluster configurations lead to a broadening of the resonances, thus lowering the detectability of cusps.

V. DISCUSSION AND CONCLUSION

Let us return to the amplitude A_{cusp} and shape of the cusps. To observe cusps, one needs to heat the Mn spin system above the bath temperature; therefore, A_{cusp} depends on $T_{\text{Mn}} - T$, which is changed by optical pumping, and on $\tau_{\text{SLR}}(B,T)$. Obviously, the dependence of these parameters on the giant Zeeman shift can explain the increase of the cusp amplitude with growing field as well as its decrease at very high fields; see Fig. 1(b). The strong shortening of τ_{SLR} for increasing x [compare Figs. 3(a) and 3(b)] also contributes to the A_{cusp} reduction. The broadening of the cusp for high Mn concentration is caused by the dispersion in the anticrossing fields due to the large number and variety of the quick-relaxing clusters as well as enhanced dipolar and exchange interactions between the single ions as a consequence of local low-symmetric crystal-field distortions. Moreover, under high optical excitation power, the relaxation rate via clusters, whose number is limited, may become insufficient, and the relaxation channel may be saturated.

The heating of the magnetic-ion spin system and an acceleration of the spin-lattice dynamics also take place in other structures besides (Zn,Mn)Se DMS QWs, such as in bulk (Cd,Mn)Te or (Cd,Mn)Se [27,34]. However, the changes observed in the SLR rates were particularly attributed to NN pair-state mixing or anisotropic exchange as the dominant mechanism of spin-pair relaxation. Strutz *et al.* [34] observed only one similar cross-resonance in (Cd,Mn)Te that corresponds to $\Delta S_{\text{total},z} = 1$, nevertheless it was not considered as a general property of the relaxation in the paramagnetic spin system. We suppose that the resonantly enhanced SLR, which is similar to our results, was not found due to the small value of the isotropic exchange constant for the NN Mn^{2+} pair as well as the negligible difference of the exchange constants for NN and NNN pairs in Cd-based DMSs, which may lead to an overlapping of different cusps and their widening by dipole-dipole interaction. In Ref. [19], the SLR inside different exchange-coupled clusters was calculated, while the idea of spin diffusion between quickly relaxing clusters and the single-ion spin ensemble was only proposed. Here, we highlight in experiment and theory the importance of the energy transfer from single spins to the spin system of NN pairs through intrinsic cross-resonances.

In conclusion, the presented results demonstrate that the Mn spin system in DMSs cannot be treated as homogeneous with respect to the SLR dynamics: the usual SLR of single magnetic ions through the phonon system is accompanied by the spin-diffusion transfer of energy to quick-relaxing centers, which are primarily pairs of antiferromagnetically coupled Mn ions in nearest-neighbor coordination. The transfer of spin and energy from the single paramagnetic ions to adjacent NN pairs is strongly enhanced by the intrinsic cross-relaxation resonances already at weak magnetic fields, where the mixing of spin levels in the complex of magnetic ions results in anticrossings. The SLR time acceleration through the mixing of states of the fast-relaxing clusters and single spins depends strongly on the perturbation strength, which mixes the crossing states, the population of these states, and the transferred magnetic-moment values. Furthermore, our results clearly highlight that the phenomenological model, which is widely used for the antiferromagnetic corrections within the modified Brillouin function, should be accomplished by a nonmonotonic $T_{\text{Mn}}(B)$ dependence to describe properly an overheated magnetic-ion spin system of small ion concentration. The magnetic resonances detected through the changes in the exciton giant spin splitting represent an alternative possibility to study spin-relaxation processes in DMSs. The disclosed SLR mechanisms can be applied to the broad class of magnetically disordered materials.

ACKNOWLEDGMENTS

This work was supported by the Deutsche Forschungsgemeinschaft in the framework of the ICRC TRR 160 and the Russian Science Foundation (Project No. 14-42-00015). V.Yu.I., J.D., and D.R.Y. acknowledge the financial support from the EAgLE project (FP7-REGPOT-2012-2013-1, Project No. 316014) for exchange visits between Dortmund and Warsaw. V.Yu.I. further acknowledges the support from the Polish National Science Center (Grant No. DEC-2014/14/M/ST3/00484).

[1] *Introduction to the Physics of Diluted Magnetic Semiconductors*, edited by J. Kossut and J. A. Gaj (Springer, Heidelberg, 2010).

[2] T. Dietl and H. Ohno, Dilute ferromagnetic semiconductors: Physics and spintronic structures, Rev. Mod. Phys. **86**, 187 (2014).

[3] J. K. Furdyna, Diluted magnetic semiconductors, J. Appl. Phys. **64**, R29 (1988).

[4] A. V. Komarov, S. M. Ryabchenko, O. V. Terletskii, I. I. Zheru, and R. D. Ivanchuk, Magneto-optical investigations of the exciton band in CdTe:Mn^{2+}, JETP **46**, 318 (1977).

[5] F. Ungar, M. Cygorek, P. I. Tamborenea, and V. M. Axt, Ultrafast spin dynamics in II-VI diluted magnetic semiconductors with spin-orbit interaction, Phys. Rev. B **91**, 195201 (2015).

[6] Y. S. Chen, M. Wiater, G. Karczewski, T. Wojtowicz, and G. Bacher, Subnanosecond magnetization dynamics induced by a pulsed magnetic field in diluted magnetic semiconductor quantum wells, Phys. Rev. B **87**, 155301 (2013).

[7] P. Olbrich, C. Zoth, P. Lutz, C. Drexler, V. V. Bel'kov, Ya. V. Terent'ev, S. A. Tarasenko, A. N. Semenov, S. V. Ivanov, D. R. Yakovlev, T. Wojtowicz, U. Wurstbauer, D. Schuh, and S. D. Ganichev, Spin-polarized electric currents in diluted magnetic semiconductor heterostructures induced by terahertz and microwave radiation, Phys. Rev. B **86**, 085310 (2012).

[8] R. Beaulac, L. Schneider, P. I. Archer, G. Bacher, and D. R. Gamelin, Light-induced spontaneous magnetization in doped colloidal quantum dots, Science **325**, 973 (2009).

[9] M. Goryca, D. Ferrand, P. Kossacki, M. Nawrocki, W. Pacuski, W. Maślana, J. A. Gaj, S. Tatarenko, J. Cibert, T. Wojtowicz, and G. Karczewski, Magnetization Dynamics Down to a Zero Field in Dilute (Cd, Mn)Te Quantum Wells, Phys. Rev. Lett. **102**, 046408 (2009).

[10] A. V. Scherbakov, A. V. Akimov, D. R. Yakovlev, W. Ossau, L. Hansen, A. Waag and L. W. Molenkamp, Spin control in heteromagnetic nanostructures, Appl. Phys. Lett. **86**, 162104 (2005).

[11] V. Yu. Ivanov, M. Godlewski, D. R. Yakovlev, M. K. Kneip, M. Bayer, S. M. Ryabchenko, and A. Waag, Optically detected magnetic resonance in (Zn, Mn)Se/(Zn, Be)Se quantum wells, Phys. Rev. B **78**, 085322 (2008).

[12] D. R. Yakovlev and I. A. Merkulov, in *Introduction to the Physics of Diluted Magnetic Semiconductors*, edited by J. Kossut and J. A. Gaj (Springer, Heidelberg, 2010), Chap. 8, pp. 263–304.

[13] H. D. Nelson, L. R. Bradshaw, C. J. Barrows, V. A. Vlaskin, and D. R. Gamelin, Picosecond dynamics of excitonic magnetic polarons in colloidal diffusion-doped $Cd_{1-x}Mn_xSe$ quantum dots, ACS Nano **9**, 11177 (2015).

[14] A. A. Maksimov, D. R. Yakovlev, J. Debus, I. I. Tartakovskii, A. Waag, G. Karczewski, T. Wojtowicz, J. Kossut, and M. Bayer, Spin diffusion in the Mn^{2+} ion system of II-VI diluted magnetic semiconductor heterostructures, Phys. Rev. B **82**, 035211 (2010).

[15] M. K. Kneip, D. R. Yakovlev, M. Bayer, A. A. Maksimov, I. I. Tartakovskii, D. Keller, W. Ossau, L. W. Molenkamp, and A. Waag, Spin-lattice relaxation of Mn ions in ZnMnSe/ZnBeSe quantum wells measured under pulsed photoexcitation, Phys. Rev. B **73**, 045305 (2006).

[16] J. Debus, A. A. Maksimov, D. Dunker, D. R. Yakovlev, E. V. Filatov, I. I. Tartakovskii, V. Yu. Ivanov, A. Waag, and M. Bayer, Heating of the Mn spin system by photoexcited holes in type-II (Zn, Mn)Se/(Be, Mn)Te quantum wells, Phys. Status Solidi B **251**, 1694 (2014).

[17] M. Blume and R. Orbach, Spin-lattice relaxation of S-state ions: Mn^{2+} in a cubic environment, Phys. Rev. **127**, 1587 (1962).

[18] Yu. G. Semenov, Interaction of a localized spin moment with phonons due to the exchange scattering of virtual carriers in semiconductors, Phys. Status Solidi B **143**, 717 (1987).

[19] D. Scalbert, Spin-lattice relaxation in diluted magnetic semiconductors, Phys. Status Solidi B **193**, 189 (1996).

[20] Y. Shapira, Magnetization steps in dilute magnetic semiconductors, J. Appl. Phys. **67**, 5090 (1990).

[21] J. Debus, D. Dunker, V. F. Sapega, D. R. Yakovlev, G. Karczewski, T. Wojtowicz, J. Kossut, and M. Bayer, Spin-flip Raman scattering of the neutral and charged excitons confined in a CdTe/(Cd, Mg)Te quantum well, Phys. Rev. B **87**, 205316 (2013).

[22] J. Debus, A. A. Maksimov, D. Dunker, D. R. Yakovlev, I. I. Tartakovskii, A. Waag, and M. Bayer, Dynamical control of Mn spin-system cooling by photogenerated carriers in a (Zn, Mn)Se/BeTe heterostructure, Phys. Rev. B **82**, 085448 (2010).

[23] The third harmonic of a Q-switched Nd:YVO_4 laser with a repetition period of 2.5 ms was used as a pump pulse. The probe density was kept below 0.01 W/cm^2 in order to avoid additional heating of the Mn spins. For the pulsed lasers, we specify the power density per pulse. The spots of the pump and probe beams with diameters of 400 μm were spatially overlapped on the sample, while their central area was selected at an intermediate image by a cross slit ($50 \times 50\,\mu m^2$).

[24] D. Keller, D. R. Yakovlev, B. König, W. Ossau, Th. Gruber, A. Waag, L. W. Molenkamp, and A. V. Scherbakov, Heating of the magnetic ion system in (Zn, Mn)Se/(Zn, Be)Se semimagnetic quantum wells by means of photoexcitation, Phys. Rev. B **65**, 035313 (2001).

[25] T. M. Giebultowicz, J. J. Rhyne, and J. K. Furdyna, Mn-Mn exchange constants in zinc-manganese chalcogenides, J. Appl. Phys. **61**, 3537 (1987).

[26] B. E. Larson and H. Ehrenreich, Anisotropic superexchange and spin-resonance linewidth in diluted magnetic semiconductors, Phys. Rev. B **39**, 1747 (1989).

[27] X. Wang, M. Dahl, D. Heiman, P. A. Wolff, and P. Becla, Spin-lattice relaxation of spin pairs in CdSe:Mn by the Dzyaloshinski-Moriya exchange interaction, Phys. Rev. B **46**, 11216(R) (1992).

[28] T. L. Estle and W. C. Holton, Electron-paramagnetic-resonance investigation of the superhyperfine structure of iron-group impurities in II-VI compounds, Phys. Rev. **150**, 159 (1966).

[29] J. K. Furdyna, M. Qazzaz, G. Yang, L. Montes, S. H. Xin, and H. Luo, Investigation of strain in II-VI semiconductor superlattices using electron paramagnetic resonance of Mn^{++}, Acta Phys. Pol. A **88**, 607 (1995).

[30] For modeling the cusp positions, it is sufficient to take into account Mn complexes with fixed inter-ion distances.

[31] We do not take into account the states connected with $S_{\text{pair}} = 2$, since these states are only weakly populated at the temperature considered.

[32] X. Wang, D. Heiman, S. Foner, and P. Becla, Magnetic-ion triplet clusters and non-nearest-neighbor exchange effect in (Cd, Mn)Te, Phys. Rev. B **41**, 1135 (1990).

[33] A. Lewicki, J. Spalek, J. K. Furdyna, and R. R. Galazka, Magnetic susceptibility of diluted magnetic (semimagnetic) semiconductors: Further evidence for superexchange, Phys. Rev. B **37**, 1860 (1988).

[34] T. Strutz, A. M. Witowski, and P. Wyder, Spin-Lattice Relaxation at High Magnetic Fields, Phys. Rev. Lett. **68**, 3912 (1992).